NUMERICAL SIMULATION OF PRESTRESSED CONCRETE NUCLEAR CONTAINMENTS

J. Cervenka[1], Z. Janda[1], D. Pryl[1]
[1]Cervenka Consulting, Ltd, Prague, Czech Republic
E-mail of corresponding author: jan.cervenka@cervenka.cz

ABSTRACT

Nuclear containments need to satisfy strong safety requirements. Computer simulation by nonlinear analysis can be used to check the structural safety, as well as to provide information about the overall load bearing capacity and reliability. Cervenka Consulting in Prague, Czech Republic develops software tools and technologies for numerical simulation of concrete structures subjected to actions due to mechanical and physical effects. Nonlinear behavior of concrete is modeled by theories of damage and plastic flow. Paper outlines the basic features of the used material model. It demonstrates the program behavior on several basic validation problems from shear concrete failure. In the last section, a nonlinear analysis is presented of the 1:4 containment model that was experimentally tested by BARC in India.

INTRODUCTION

Computer modeling of reinforced concrete structures must reflect all typical features exhibited by brittle cementitious materials, reinforcement and their interactions due to bond. The numerical model of reinforced concrete is usually complex, and is a result of numerous approximations. It is essential to employ a balanced approximation approach, in which the resulting response guarantees a good agreement with the real behavior. This can be assured by a quality control system based on validation. Such validation should include comparison with experiments, blind bench mark tests, effects of numerical methods, namely criteria for iterative procedures and mesh sensitivity.

Validation is briefly discussed in the first part of the paper along with the main principles of the employed material models. An application of ATENA to containment analysis are shown in the second part of the paper

MATERIAL MODEL FOR CONCRETE

Material model for concrete in ATENA is based on the smeared crack model for tension combined with plasticity model for compression. Model is described in detail in the paper by Červenka & Pappanikolaou [3]. The material model formulation assumes small strains, and is based on the strain decomposition into elastic (ε_{ij}^{e}), plastic (ε_{ij}^{p}) and fracture (ε_{ij}^{f}) components. The stress development can be then described by the following rate equations describing the progressive degradation (concrete cracking) and plastic yielding (concrete crushing):

$$\dot{\sigma}_{ij} = D_{ijkl} \cdot (\dot{\varepsilon}_{kl} - \dot{\varepsilon}_{kl}^{p} - \dot{\varepsilon}_{kl}^{f}) \tag{1}$$

The constitutive equations of the both models can be summarized as follows:

Flow rule governs the evolution of plastic and fracturing strains:

Plastic model: $$\dot{\varepsilon}_{ij}^{p} = \dot{\lambda}^{p} \cdot m_{ij}^{p}, \; m_{ij}^{p} = \frac{\partial g^{p}}{\partial \sigma_{ij}} \tag{2}$$

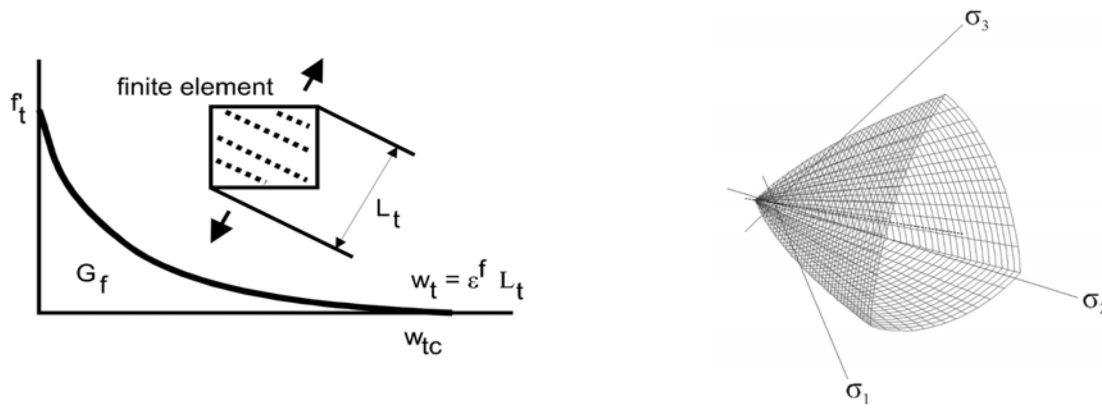

(a) Tensile softening (Hordijk 1991) (b) Three paramater criterion for concrete (Menetrey & Willam 1995)

Fig. 1: Material law for concrete in tension and compression

$$\text{Fracture model:} \quad \dot{\varepsilon}^f_{ij} = \dot{\lambda}^f \cdot m^f_{ij},\ m^f_{ij} = \frac{\partial g^f}{\partial \sigma_{ij}} \tag{3}$$

Where $\dot{\lambda}^p$ is the plastic multiplier rate and g^p is the plastic potential function. Following the unified theory of elastic degradation of Carol et al. [5] it is possible to define analogous quantities for the fracturing model, i.e. $\dot{\lambda}^f$ is the inelastic fracturing multiplier respectively and g^f is the potential defining the direction of inelastic fracturing strains in the fracturing model. The consistency conditions can be than used to evaluate the change of the plastic and fracturing multipliers.

$$\dot{f}^p = n^p_{ij} \cdot \dot{\sigma}_{ij} + H^p \cdot \dot{\lambda}^p = 0\,,\ n^p_{ij} = \frac{\partial f^p}{\partial \sigma_{ij}} \tag{4}$$

$$\dot{f}^f = n^f_{ij} \cdot \dot{\sigma}_{ij} + H^f \cdot \dot{\lambda}^f = 0\,,\ n^f_{ij} = \frac{\partial f^f}{\partial \sigma_{ij}} \tag{5}$$

H^p and H^f are hardening/softening moduli for plastic model and fracturing model, respectively. This represents a system of two equations for the two unknown multiplier rates $\dot{\lambda}^p$ and $\dot{\lambda}^f$, and is analogous to the problem of multi-surface plasticity (Simo et al. [9]). The details of the model implementation can be found in Červenka & Pappanikolaou [3]. The model is using Rankine criterion for tensile fracture with exponential softening of Hordijk [6], see Fig. 1(a).

The compressive behavior is modeled by a plasticity model, which is using the three parameter surface of Menetrey & Willam [8] (see Fig. 1(b). The softening in tension and compression is adjusted using a crack band approach of Bažant & Oh [1]. The crack band L_t as well as crush band size L_c are adjusted with regard to the crack orientation by Eq.(6), where θ is the angle between crack direction and average orientation of element.

$$L'_t = \gamma L_t \ \text{ and } \ L'_c = \gamma L_c\,,\ \gamma = 1 + (\gamma_{max} - 1)\frac{\theta}{45},\ \ \theta \in \langle 0; 45 \rangle\,,\ \gamma_{max} = 1.5 \tag{6}$$

The basic idea is to adjust the crack band size depending on the crack orientation with respect to the element edges or surfaces in 3D. This reflects the fact that a crack cannot localize into a single element if the crack direction is not aligned with the element edges.

Concrete constitutive model covers also functions related to the shear resistance of cracks and reduction of compressive resistance due to cracking, which are important for realistic modeling of cracked concrete, Bentz et al. [2].

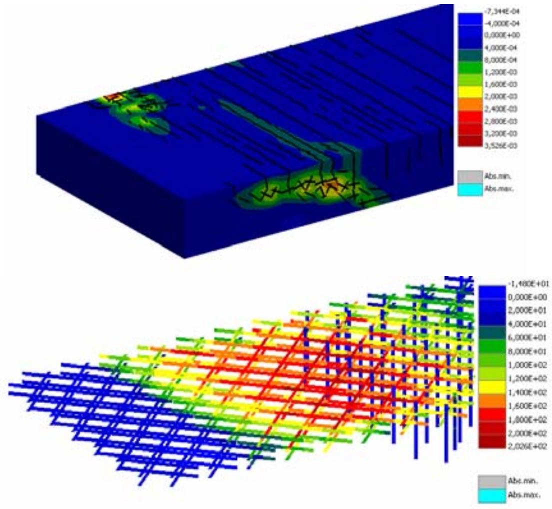

(a) Slab shear test at ETH Zurich 2005

(b) ATENA simulation slab tests, above: crack pattern , below: bar stress

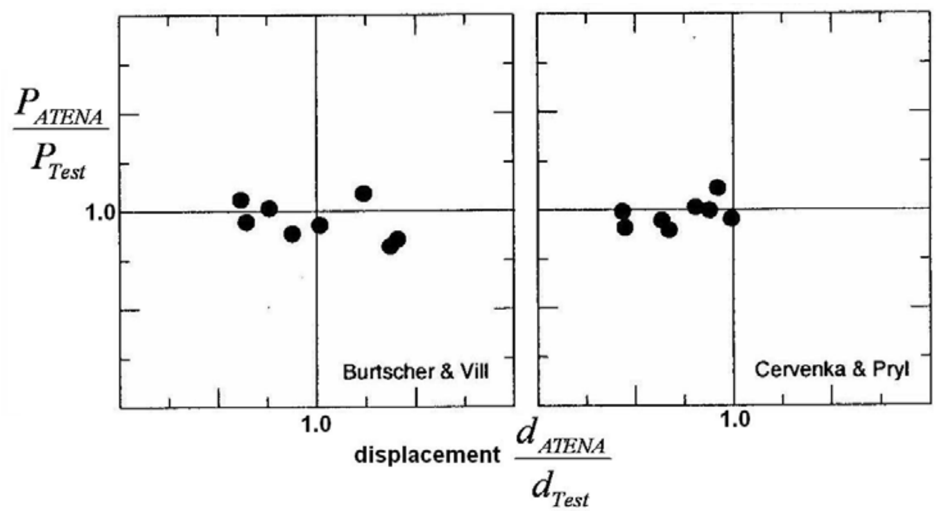

(c) ATENA prediction results of two teams

Fig. 2: Prediction competition of slab shear resistance

VALIDATION

It is essential to validate numerical models by comparing with experimental results and ATENA has been tested by many such studies. One example was a prediction of shear response of RC slabs organized by Marti at ETH Zurich (Jeager and Marti [7]). Slab reinforcement was inclined with respect to bending direction making effect of crack orientation with respect to reinforcement an important issue. Right estimation of three-dimensional mechanics of cracked concrete was essential for correct prediction of shear resistance.

Test arrangement overview is shown in Fig. 2(a) and illustration of ATENA simulation is shown in Fig. 2(b). Fig. 2(c) shows the strength prediction for two ATENA analyses by two independent participants: Wiena

University and Cervenka. The prediction value is measured by the ratio of predicted and tested strength on vertical axis and displacements at failure is on the horizontal axis. In this representation, the exact prediction would be in the graph centre. It can be seen that strength predictions was remarkably well predicted by both independent teams.

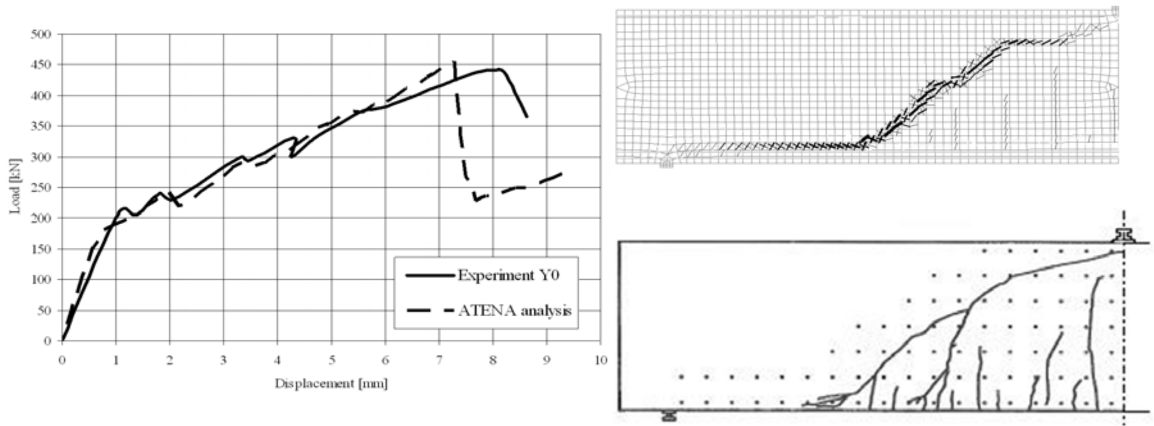

(a) Beam Y0 without shear reinforcement

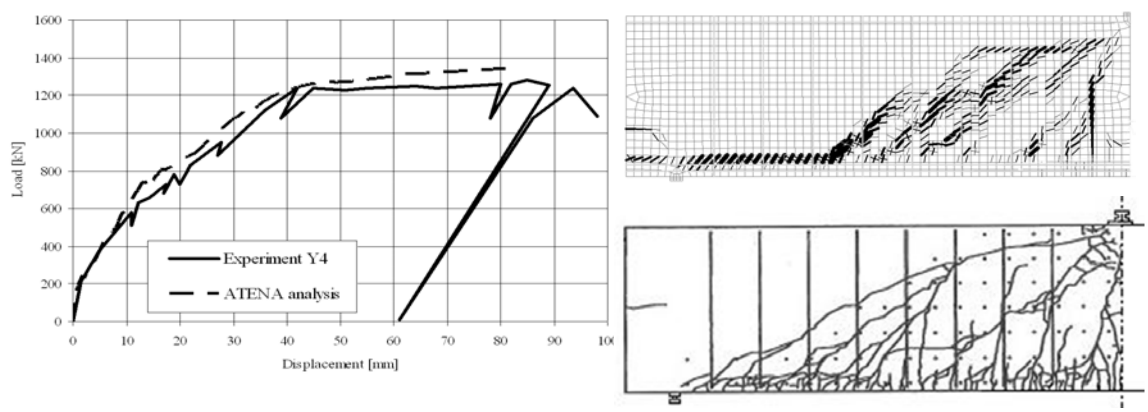

(a) Beam Y4 with shear reinforcement

Fig. 3: Simulation of shear failure of large shear beams tested by Collins&Yoshida 2005

Second example shows comparison of ATENA simulation of shear resistance of large beams tested by Collins and Yoshida. Fig. 3 shows two beams, dimensions depth 2 m, length 12 m, with and without vertical shear reinforcement. Ultimate loads as well as failure patterns in both cases were closely simulated by ATENA. Due to large dimensions a size effect was significant and well reflected by ATENA calculation. Remarkable is the effect of shear reinforcement. In beam with only slight shear reinforcing ratio 0.00071 the ultimate load increased almost by factor 3. Also a significant increase in ductility is observed both in the experiment as well as in the simulation. The failure in beam Y0 was brittle due to inclined crack, while in the beam Y4 a combine bending-shear failure occurred.

BARCOM ROUND ROBIN ANALYSIS

Concrete containment model in the scale of 1:4 was tested in BARC laboratories in India, (Fig. 4), in order to provide data for validation of analysis methods and software for design of containments in NPP. The numerical model of the test containment is shown in Fig. 4 (right). The containment concrete has a strength grade C45.

Reinforcement material has yield stress of 550 MPa. Pre-stressing cables are stretched up to 80% of their minimum guaranteed ultimate tensile strength (UTS) 1848 MPa.

Fig. 4: Model containment tested in BARC (left) and its numerical model (right)

(a) walls (b) ribs (c) cables

Fig. 5: Elements of numerical model

Efficient numerical model need to combine various finite element types as shown in Fig. 5. Walls and dome are modeled by special three-dimensional layered shell elements (Fig. 5(a)), which allow a significant reduction of the model size, while maintaining very good approximation of the stress state. The vertical ribs and the ring for anchoring of prestressing cables and the foundation slab are modeled by high order solid elements (Fig. 5(b). Two types of models are used for reinforcement. Ordinary non-prestressed reinforcement is modeled by smeared reinforcement and for prestressing cables discrete bar elements are used (Fig. 5(c)). Altogether the numerical model consisted in this case of 17031 elements, which made it possible to perform a global containment analysis in reasonable time with sufficient accuracy.

The analysis was performed for a test under increasing internal air pressure up to failure. In the first 10 steps only dead load is applied to the model. In the subsequent 10 steps, the pre-stressing is applied as an initial strain in the tendon cables. The final initial pre-stressing load is 80% of 26.6Tons/cable. This means a pre-stressing force of 21.3 Tons/cable, i.e. a tendon pre-stressing of 1490 MPa. This pre-stressing is applied as an initial tendon strain of 7.6‰. After that an internal pressure is gradually applied on the interior concrete wall. At this point the solution method is changed from Newton-Raphson to Arc-length. The internal pressure is being gradually increased up to the level when the pre-stressing tendons start to rupture.

At the end of pre-stressing minor micro cracks appear at the locations with high stress concentration. This is just below the ring and at the location, where the wall is connected to the foundation slab.

Subsequently the model is loaded by an inner pressure, which simulates the proposed pressure test. During the pressure loading the containment remains largely in the elastic domain almost up to the pressure level of 200% Pd. Up to this load level only minor concrete cracking is observed near the ring as well as at the bottom parts of the wall, near the widening of the bottom wall parts. A significant crack growth starts at approximately (240-250% of the design pressure - Pd). At this load level significant horizontal cracks appear in the ring and at the bottom of the wall and vertical cracks in the mid of the containment wall. The first load peak is situated in step 46 (260% of Pd), when a quick grow of radial cracks is evident in the model. The radial cracks start to propagate from the bottom part of the containment wall. In the subsequent steps the radial crack propagates through the whole height of the wall (Fig. 6). In approximately 275% of Pd the tendon yielding starts. The ultimate load capacity according to the axi-symmetrical analysis is reached at the level of 320-350% of Pd (i.e. the pressure of 0.4946 MPa). At this load level the vertical tendons at the bottom of the wall reach their strain elongation capacity and may start to rupture.

The ultimate load capacity according to the three-dimensional analysis is reached at 329% of Pd (i.e. the pressure of 0.4648 MPa).

The load-displacement diagram from the ATENA analyses is shown in Fig. 6. The ultimate pressure is determined mainly by yielding of prestressing cables and reinforcement near openings. The global safety factor obtained by the analysis was 3.2 times the design pressure of 0.14 MPa.

The limit load is determined mainly by yielding of pre-stressing cables in the vicinity of structural holes. The global safety factor calculated by the numerical simulations is about 3.2 due to the pressure head of 0.140 MPa. Fig. 7 and 8 shows graphs of LD diagrams of all participants on these experiments. ATENA results are indicated by a small arrow approximately in the middle of all results.

Six experimental tests have already been performed at BARC when this article was prepared. Tests #1 to #4 were up to 100% of design pressure. Test #5 and 6 were up to 156% of the design pressure. Fig. 9 shows the displacements at dome crown from these tests. Next tests (increase loading up to failure) should take place in 2011 in the laboratories of BARC, and the results will be probably available at the time of the conference.

Fig. 6 shows the deformed shape and cracks at maximum pressure. This figure also depicts the unique capabilities of the software for realistic visualization of material cracking.

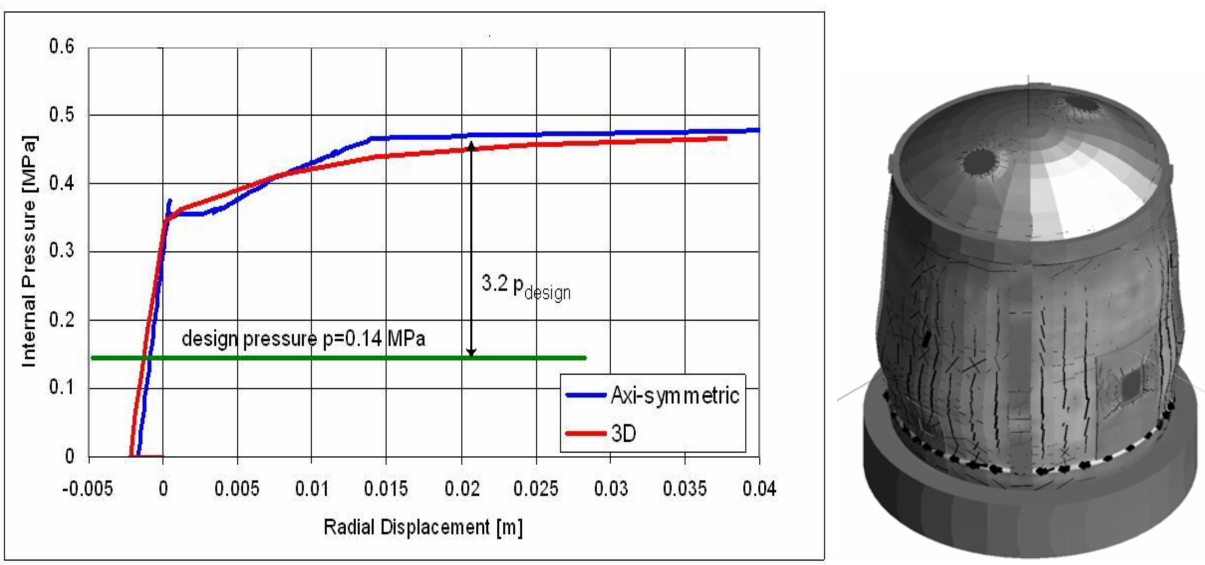

Fig. 6: Diagram of the pressure-radial displacement. Deformed shape at failure.

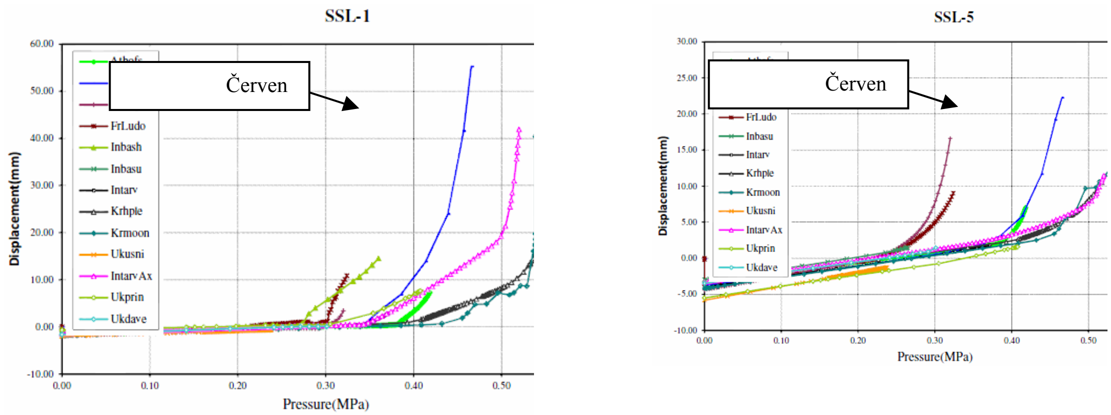

(a) LD diagrams bottom of wall. (b) LD diagrams at dome crown.

Fig. 7: Load displacement diagrams of various participants

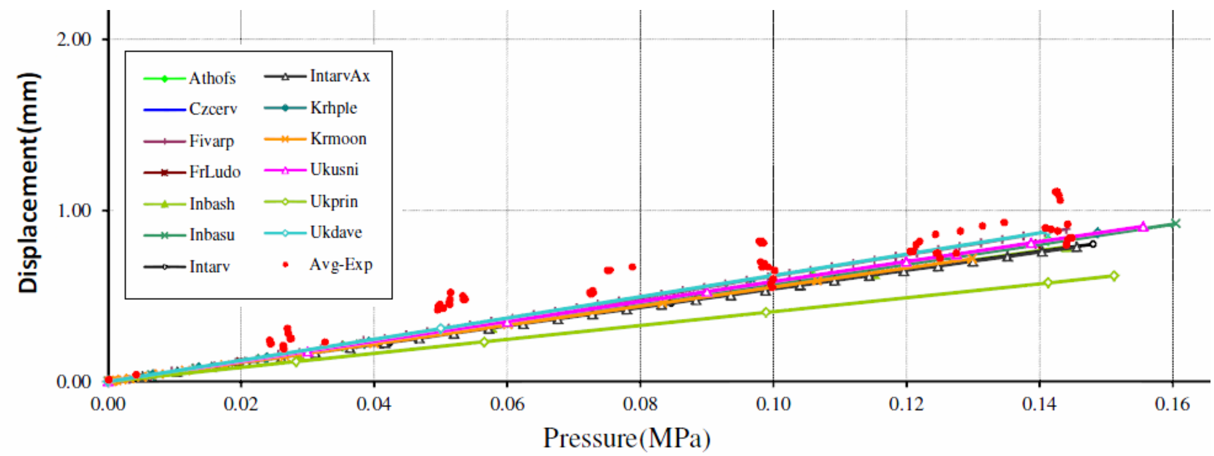

Fig. 8: Comparison of all participants with experimental data in the elastic range

CONCLUSIONS

Nonlinear analysis is a useful tool for safety assessment of nuclear containment structures. In the modern design approach, it is becoming a standard procedure to verify the structural safety by a nonlinear simulation. This is especially necessary for structures requiring high safety margin such as nuclear containments.

The nonlinear simulation is a global assessment approach, which requires an application of global safety formats. Such formats are now becoming available in modern design standards such as for instance Eurocodes or the new model code from fib (fib – model code 2010).

ATENA software supports these modern design approaches, and has been specifically developed for the analysis of reinforced concrete structures with strong emphasis on easy and robust modeling of reinforcement. The material models for concrete are designed to capture the main aspect of the brittle material behavior, and are extensively tested by experiments and blind prediction competitions.

Models presented in the paper were developed in research project CERHYD FR-TI1/612 supported by Czech Ministry of Industry and Commerce and project P105/10/1156 supported by Czech grant agency.

REFERENCES

[1] Bažant, Z.P., Oh, B.H., 1983. Crack band theory for fracture of concrete. Materials and Structures, RILEM 16

[2] Bentz, E.C., Vecchio, F.J., Collins, M.P. 2006. Simplified Modified Compression Field Theory for Calculating Shear Strength of Reinforced Concrete Elements. ACI Material Journal, Jul/Aug 2006.

[3] Cervenka, J., Pappanikolaou, V. 2008, Three dimensional combined fracture-plastic material model for concrete. Int. J. of Plasticity, Vol. 24, 12, 2008, ISSN 0749-6419, pp. 2192-2220

[4] Collins, M.P., Vechio, F., Mehlhorn, G. 1983 – An International Competition to Predict the Response of Reinforced Concrete Panels, Festschrift Prof. Dr. Bruno Thurlimann, ETH Zurich, pp. 471-491

[5] Carol, I., Rizzi, E., Willam, K., 1994. A unified theory of elastic degradation and damage based on a loading surface. International Journal of Solids and Structures 31 (30), 2835-2865.

[6] Hordijk, D.A. 1991. Local approach to fatigue of concrete. PhD Thesis, Delft University of Technology, The Netherlands.

[7] Jaeger, T., and Marti, P., “Versuche zum Querkraftwiderstand und zum Verformungsvermögen von Stahlbetonplatten (Tests on the shear strength and the deformation capacity of reinforced concrete slabs)”, Report No. 294, Institute of Structural Engineering, ETH Zurich, February 2006, 358pp.

[8] Menétrey, P., Willam, K.J. 1995. Triaxial failure criterion for concrete and its generalization. ACI Structural Journal 92 (3), 311-318.

[9] Simo, J.C., Kennedy, J.G., Govindjee, S., 1988. Non-smooth multisurface plasticity and viscoplasticity. Loading/unloading conditions and numerical algorithms. International Journal for Numerical Methods in Engineering 26 (10), 2161-2185.

[10] fib – Model Code 2010, federation internationale du beton, 2010, bulletin 56, ISBN 978-2-88394-096-3